Journal of Translational Autoimmunity 10 (2025) 100265

Contents lists available at ScienceDirect

Journal of Translational Autoimmunity

journal homepage: www.sciencedirect.com/journal/journal-of-translational-autoimmunity

The role of UV-induced cutaneous matrix metalloproteinases and mi-RNAs in the pathogenesis of lupus erythematosus

I. Ivanova, T. Svilenska, T. Maisch, S. Karrer, D. Niebel, M. Berneburg, B. Kurz *

Department of Dermatology, University Medical Center Regensburg, 93042, Regensburg, Germany

ARTICLE INFO

Handling editor: Y Renaudineau

Keywords:
Lupus erythematosus
Matrix metalloproteinases
Metabolism
Mi-RNAs

ABSTRACT

Cutaneous (CLE) and systemic lupus erythematosus (SLE) are autoimmune diseases with a multifactorial pathogenesis. Ultraviolet radiation (UVR) is the most important trigger of CLE; however, the degree of photosensitivity varies between the clinical subtypes. The expression of matrix metalloproteinases (MMPs)—important enzymes involved in skin turnover and homeostasis—is modulated by UVR.

To investigate the causality of the clinically observed effects of UVR, sun-exposed lesional skin samples from patients with different subtypes of lupus erythematosus (LE) were examined by immunohistochemistry for the expression of MMP1 and MMP28 and compared with biopsies from polymorphous light eruption (PLE) and healthy skin (HS). The expression of micro-RNAs (miR-31 and miR-150)—regulators of MMP expression and cellular metabolism—in the samples was determined by in-situ hybridization and correlated with the expression of the glucose transporter 1 (GLUT1) receptor to examine potential metabolic regulation. To assess potential UVR regulation of MMP28, we performed *in vitro* experiments in healthy keratinocytes and fibroblasts.

MMP28 expression was differentially affected by UVA1 and UVB irradiation in keratinocytes and fibroblasts. Compared with all other LE subtypes, as well as PLE and HS samples, MMP28 expression in Chilblain LE skin showed a distinct vertical distribution, reaching as far as the upper layers of the dermis. This vertical expression pattern coincided with decreased GLUT1 levels and with increased expression of miR-31 and miR-150 in the epidermis of patients with Chilblain LE. These data provide evidence for a potential metabolic dysregulation that may play a role in the etiology of LE. Furthermore, our results suggest MMP28 as a novel complementary marker in Chilblain LE diagnosis.

1. Introduction

Cutaneous (CLE) and systemic lupus erythematosus (SLE) are ultraviolet-A (UVA) (315–400 nm) and ultraviolet-B (UVB) (280–315 nm) radiation-associated autoimmune diseases with an incidence of 0.3/100,000 person-years in Africa and up to 23.2/100,000 person-years in North America [1]. Clinical manifestations of LE range from mild, such as skin-only disease in CLE, to severe and potentially life-threatening in SLE [2,3]. SLE is defined according to the 1982 criteria of the American College of Rheumatology [4] and the revised version of The Systemic Lupus Erythematosus International Collaborating Clinics criteria [5]. CLE is defined as isolated cutaneous lupus lesions occurring in the absence of significant evidence of SLE and is further subdivided into acute cutaneous lupus erythematosus (ACLE), subacute cutaneous lupus erythematosus (SCLE), chronic cutaneous lupus erythematosus (including discoid lupus erythematosus (DLE)), LE tumidus (LET), and Chilblain lupus. The pathogenesis of both CLE and SLE is multifactorial and includes genetic predisposition, environmental triggers, and abnormalities in the innate and adaptive immune response. The current view is that UV radiation (UVR) triggers cell damage and apoptosis, with LE being more sensitive to UVB than to UVA. Furthermore, T cell dysregulation, cytokine imbalances, B cell defects, and autoantibody

Abbreviations: **ACLE**, acute cutaneous lupus erythematosus; **ACR/EULAR**, American College of Rheumatology/European League Against Rheumatism; **CLE**, cutaneous lupus erythematosus; **DLE**, discoid lupus erythematosus; **GLUT1**, glucose transporter 1; **HS**, healthy skin; **ICH**, immunohistochemistry; **IL**, interleukin; **LE**, lupus erythematosus; **LET**, lupus erythematosus tumidus; **miR-31/miR-150**, micro-RNA 31/ micro-RNA 150; **mi-RNA**, micro-RNA; **MMP**, matrix metalloproteinase; **mRNA**, messenger RNA; **PBS**, phosphate-buffered saline; **PLE**, polymorphous light eruption; **SCLE**, subacute cutaneous lupus erythematosus; **SLE**, systemic lupus erythematosus; **UV**, ultraviolet; **UVR**, ultraviolet radiation.

* Corresponding author.
E-mail address: Bernadett.Kurz@ukr.de (B. Kurz).

https://doi.org/10.1016/j.jtauto.2024.100265
Received 25 November 2024; Received in revised form 24 December 2024; Accepted 27 December 2024
Available online 28 December 2024

production seem to contribute to the development of LE [2].

The pathogenesis of LE involves impaired keratinocyte clearance, inflammatory events, and an impaired immune response that may be mediated by the altered expression of various matrix metalloproteinases (MMPs). MMPs are markers of UV-induced skin damage and, as proteinases, are responsible for the degradation of extracellular matrix proteins and contribute to UV-induced skin aging [6]. They also play a crucial role in photocarcinogenesis by regulating processes related to tumor progression, including tissue homeostasis as well as tumor vascularization, invasion, and metastasis [7]. Since MMP expression is regulated by UVR, MMPs may also play a role in the pathogenesis of LE [8]. High intrathecal and serum MMP9 levels have been found in SLE patients with neuropsychiatric symptoms [9], and the upregulation of this protein may be responsible for the vascular damage in peripheral neuropathy of SLE [10]. MMP1 (UVA and UVB regulated) and MMP9 (UVA and UVB regulated) activity is increased in the serum of SLE patients and may be associated with inflammatory activity [11,12]. In addition, SLE patients show elevated serum and plasma levels of MMP3, which may contribute to vascular wall damage in SLE neuropathy and in the pathogenesis of lupus nephritis [13]. Elevated MMP2 (UVA and UVB regulated) and MMP9 levels have previously been found in lesional CLE skin and have been shown to correlate with disease activity [14].

In contrast to other MMPs, the role of MMP28 in LE is still unclear. MMP28 is physiologically expressed in keratinocytes to promote wound healing and tissue homeostasis [15]. It has been suggested that disruption of the clearance of UV-induced apoptotic keratinocytes may play a role in LE inflammation [16], thus making MMP28— an epilysine important for tissue homeostasis [17,18]—a suitable target for further research in LE. Taken together, these findings suggest that MMPs play an important role in the initiation and progression of inflammation and tissue damage in both CLE and SLE.

UVR not only induces changes in the expression of MMPs but also affects micro-RNAs (mi-RNAs) [19,20]. Mi-RNAs are a large group of short, non-coding RNA molecules involved in the post-transcriptional control of gene expression [21]. Their effects are exerted by base pairing with messenger RNA (mRNA), resulting in enhanced mRNA decay and/or attenuation of translation [22,23]. Mi-RNAs may be up- or down-regulated in autoimmune diseases such as LE and may also be affected by UVR. So far, mi-RNAs have been studied predominantly in cell culture and serum from LE patients and rarely in lesional skin.

Among others, miR-31 showed lower expression in the plasma of SLE patients and higher expression in in-situ hybridization of CLE patient tissue. Dysregulation of miR-31 and its target Ras homolog family member A (RhoA) could be a novel molecular mechanism underlying the IL-2 deficiency in patients with SLE [24]. Overexpression of miR-31 contributes to skin inflammation in DLE lesions by regulating the production of inflammatory mediators such as interleukin (IL)-1β, IL-12, and IL-8 in keratinocytes and by attracting neutrophils and intermediate monocytes to the skin [25]. Besides its proinflammatory function, miR-31 also interacts with MMP1 to promote epithelial-to-mesenchymal transition [26]. Furthermore, miR-31 is known to regulate glucose metabolism through the glucose transporter 1 (GLUT1) receptor [27]. Cell culture experiments have shown that UVA and UVB upregulate miR-31 levels [20].

Pro-inflammatory miR-150 showed higher expression in patients with SLE [28] but lower expression in patients with CLE [29]. Regarding the critical role of miR-150 in skin biology, its downregulation has been shown to promote keratinocyte proliferation under hypoxic conditions by targeting hypoxia-inducible factor 1-alpha (HIF-1α) and vascular endothelial growth factor A (VEGF-A). Downregulation of miR-150 in CLE may influence the activation of chronic inflammatory and pro-fibrotic pathways [29]. So far, it is not clear whether miR-150 is UVA and/or UVB regulated. Similar to miR-31, miR-150 can negatively regulate GLUT1 expression in psoriasis and osteosarcoma [27,30] to interfere with cellular glucose metabolism.

In the context of LE, an upregulation of GLUT1 has already been observed in patients with SLE [31]. Inhibition of GLUT1 using T cell-specific knockouts or small molecules that inhibit glycolysis has already improved the phenotypes of several murine autoimmune disease models, such as arthritis, LE, and psoriasis. Deletion or inhibition of GLUT1 blocked T cell proliferation and effector function, antibody production by B cells, and reduced the inflammatory responses in macrophages [32].

The objective of the current study was to investigate the differences in molecular patterns associated with UV exposure in CLE subtypes and SLE. As such, emphasis was put on MMPs (namely MMP1 and MMP28) as drivers of tissue remodeling and homeostasis, and the glucose transporter GLUT1 as regulator of MMP expression. We also wanted to investigate possible aberrations in the skin patterns of miR-31 and miR-150 in LE patients, considering their role in GLUT1 and immune response modulation. As a final outcome, we hoped identify distinct marker combinations that could help to better differentiate between the subtypes of LE and even serve as foundation for improving the currently available LE treatment strategies.

For this reason, skin biopsies from patients with CLE and SLE were immunohistochemically analyzed for the expression of MMP1, MMP28, and GLUT1. Furthermore, we used keratinocyte and fibroblast cell cultures to assess MMP28 regulation before and after UVA1 and UVB irradiation. Finally, we examined via base scope miR-31 and miR-150 and their correlation with MMP28 and GLUT1 expression patterns in patients with CLE and SLE compared to polymorphic light eruption (PLE) and healthy skin (HS).

2. Materials and methods

2.1. Acquisition of histological samples from lupus erythematosus patients and healthy controls

We retrospectively analyzed paraffin-embedded skin biopsies that had been taken consecutively from 2010 to 2022 from 49 patients with CLE, SLE, and a control group with PLE (n = 5) and HS (n = 3). Skin biopsy specimens were taken from untreated lesions on sun-exposed body sites (fingers, arms, thorax, or scalp) of all patients with LE or PLE. The study population included patients with ACLE (n = 3), SCLE (n = 12), DLE (n = 11), LET (n = 10), Chilblain LE (n = 10), and SLE (n = 3). The subtype of CLE was defined according to clinicopathologic correlation. SLE diagnosis was made when at least 4 of the revised SLE criteria of the ACR/EULAR (American College of Rheumatology/European League Against Rheumatism) were present. All patients underwent a medical history, physical examination, and routine blood analysis. Biopsies from 5 patients with PLE and 3 patients without skin disease (healthy donors) were used as controls.

2.2. Immunohistochemistry staining

2.2.1. Deparaffinization of histological samples prior to immunohistochemistry staining

Immunohistochemistry (IHC) was performed on formalin-fixed and paraffin-embedded skin samples, from which 2 μm sections were used. For all immunohistochemistry staining procedures, the samples were dried at 60 °C for 1h and deparaffinized in a descending alcohol series as follows: 3 × 10 min xylene, 2 × 5 min 100 % ethanol, 2 × 5 min in 96 % ethanol, and 1 × 5 min 70 % ethanol. The subsequent staining steps are described below individually for each antibody.

2.2.2. Immunohistochemistry staining of MMP28

After deparaffinization and rehydration, the sections were incubated with 3 % H_2O_2 (in ethanol) for 10 min to block unspecific reactions. After a brief wash in dH_2O, the slides were placed in a steamer in citrate buffer (pH 6) (Zytomed Systems GmbH, Germany) for 20 min, followed by 30 min cooling to room temperature and a brief wash in H_2O. Tissue sections were contoured with an ImmEdge barrier pen (Vector

Laboratories, USA). The tissue slides were incubated in blocking solution (Zytomed Systems GmbH, Germany) for 10 min, rinsed in phosphate-buffered saline (PBS) for 5 min, and incubated with an anti-MMP28 antibody (1:400 dilution, PA5-100157, Thermo Fisher Scientific, USA) overnight at 4 °C. After 5 min washing with PBS, slides were incubated in an anti-rabbit Histofine® (Medacshop, Hamburg, Germany) at room temperature for 30 min, rinsed in PBS for 5 min, and incubated with AEC substrate chromogen (ready-to-use; Dako/Agilent, USA) at room temperature. The staining reaction was stopped with H_2O, and counterstaining was performed with hematoxylin. Aquatex (Sigma-Aldrich/Merck, Germany) was used for mounting the coverslips.

2.2.3. Immunohistochemistry staining of MMP1

After deparaffinization and rehydration, the tissue sections were incubated with 3 % H_2O_2 (in ethanol) for 10 min to block unspecific reactions. After a brief wash in dH_2O, the slides were placed in a steamer in citrate buffer (pH 6) (Zytomed Systems GmbH, Germany) for 20 min, followed by 30 min cooling to room temperature and a brief wash in H_2O. Tissue sections were contoured with an ImmEdge barrier pen (Vector Laboratories, USA). The tissue slides were incubated in blocking solution (Zytomed Systems GmbH, Germany) for 10 min, rinsed in PBS for 5 min, and incubated with an anti-MMP1 antibody (1:200 dilution; IMG-80426, Imgenex/Novus Biologicals, USA) overnight at 4 °C. After 5 min washing with PBS, slides were incubated with an anti-rabbit secondary antibody (Zytomed Systems GmbH, Germany) at room temperature for 30 min. Samples were washed again with PBS and incubated with an HRP-conjugate (Zytomed Systems GmbH, Germany) at room temperature for 30 min. After a final washing step, the samples were incubated with AEC substrate chromogen (ready-to-use; Dako/Agilent, USA). The staining reaction was stopped with H_2O, and counterstaining was performed with hematoxylin. Aquatex (Sigma-Aldrich/Merck, Germany) was used for mounting the coverslips.

2.2.4. Immunohistochemistry staining of GLUT1

After deparaffinization and rehydration, the sections were placed in a steamer in Tris-EDTA buffer (pH 9) (Zytomed Systems GmbH, Germany) for 20 min, followed by a 30 min cooling to room temperature and a brief wash in H_2O. Tissue sections were contoured with an ImmEdge barrier pen (Vector Laboratories, USA). The tissue slides were incubated in blocking solution (Zytomed Systems GmbH, Germany) for 10 min, rinsed in PBS for 5 min, and incubated with an anti-GLUT1 antibody (1:500 dilution; ab115730, Abcam, UK) overnight at 4 °C. After a 5-min wash with PBS, slides were incubated with an anti-rabbit secondary antibody (Zytomed Systems GmbH, Germany) at room temperature for 30 min. Samples were washed again with PBS and incubated with an HRP-conjugate (Zytomed Systems GmbH, Germany) at room temperature for 30 min. After a final washing step, the samples were incubated with AEC substrate chromogen (ready-to-use; Dako/Agilent, USA). The staining reaction was stopped with H_2O, and counterstaining was performed with hematoxylin. Aquatex (Sigma-Aldrich/Merck, Germany) was used for mounting the coverslips.

2.2.5. Scoring of the immunohistochemistry staining for MMP1, GLUT1, and MMP28

Experienced dermatopathologists from the Department of Dermatology visually evaluated the immunohistochemically stained samples by applying the immuno-reactive score described in Table 1.

In MMP28 staining, the vertical distribution of the marker in the histological samples was determined. The skin sections were subdivided into upper epidermis, whole epidermis without *Stratum (S.) basale*, whole epidermis with *S. basale* and dermis; the marker distribution was assessed and scored in accordance with Table 2.

2.2.6. Imaging of the immunohistochemistry samples

Images of the immunohistochemical stainings were taken at 40x and 20x magnification using BZ-X810 inverted combined fluorescence and phase contrast microscope (Keyence, Germany). BZ-H4C imaging software (Keyence, Germany) was implemented in the process.

Table 1
Immuno-reactive score, calculation of marker expression, and assigned numerical values for the IHC staining of MMP1 and GLUT1.

A: Percentage of tissue stained	B: Intensity of the stain	Evaluation of results (AxB)	Assigned numerical value for statistical calculations
0–0 %	0 – no stain	0-1 negative	0
1 – <10 %	1 – weak	2 very weakly positive	1
2–10-50 %	2 – mild	3-4 weakly positive	2
3–51-80 %	3 – strong	6-8 moderately positive	3
4 – >80 %		9-12 strongly positive	4

The immuno-reactive score was derived from the publications of Fedchenko et al., 2014 and Remmele et al., 1987 [33,34].

Table 2
Numerical scores for the vertical distribution of MMP28 following the IHC staining.

Extent	Assigned numerical value for statistical calculation
Upper epidermis only (inclusive *Stratum granulosum*)	1
Whole epidermis without *S. basale*	2
Whole epidermis with *S. basale*	3
Epidermis, *S. basale* and dermis	4

2.3. miRNA in situ hybridization of miR-31 and miR-150

2.3.1. Sample preparation for in situ hybridization

In situ hybridization was performed on 4-μm histological samples using the Base Scope System (Advanced Cell Diagnostics/Biotechne, USA). The probes for two micro RNAs miR-31 (catalog number: 712631) and miR-150 (catalog number: 710111) were hybridized according to the manufacturer's protocol, but with a slight modification. A PPIB probe was used as a hybridization control.

Tissue permeabilization was performed with Protease IV (Advanced Cell Diagnostics/Biotechne, USA) at 40 °C for 30 min. Probe hybridization was carried out in a Twin Tower Block of a PTC-200 DNA Engine Cycler (Bio-Rad, Germany). The hybridization process followed the manufacturer's protocol for a Base Scope Detection Kit v2 RED (Advanced Cell Diagnostics/Biotechne, USA) up to the AMP7 hybridization step, in which the incubation time was set to 1 h at room temperature. After incubation with AMP8 and a washing step in accordance with the standard protocol, the slides were incubated in a Base Scope Fast RED substrate at room temperature for 15 min. Subsequently, the slides were washed, counterstained with hematoxylin, dried at 60 °C for 1 h, and mounted with VectaMount (Vector Laboratories, USA).

2.3.2. In situ hybridization scoring

An overview of each section was acquired at 10x magnification with BZ-X810 inverted combined fluorescence and phase contrast microscope (Keyence, Germany). Since hybridization was observed exclusively in the epidermis, the area of the epidermis was calculated with ImageJ 1.54d (National Institute of Health, USA) and given in [mm^2]. Serial images of the complete epidermis were made for each sample at 40x magnification, and the number of positive hybridization events (dots) was counted semi-quantitatively. The final hybridization results are presented as [dots/mm^2].

2.4. Cell culture

2.4.1. Isolation and culturing of healthy primary human fibroblasts (Re5)

A healthy skin biopsy sample obtained from the University Medical Center Regensburg was given the designation Re5 and was used for harvesting primary human fibroblasts. The skin biopsies were placed on a Primaria cell culture dish (Corning, Germany) with a single drop of DMEM-Cipro medium (DMEM medium (P04-01548, PAN Biotech, Germany) containing 10 % FCS (Anprotec, Germany), 1 g/L (5.5 mM) glucose (Sigma-Aldrich/Merck, Germany), 1 mM pyruvate (Thermo Fischer, Germany), and 2 mM L-glutamine (Sigma-Aldrich/Merck, Germany), Ciprofloxacin 1 % (200 mg/100 mL infusion solution, Fresenius Kabi, Germany). The samples were and incubated at 37 °C for 30 min to ensure that the skin sample adhered to the dish surface. Afterward, 3 mL DMEM-Ciprofloxacin was added to the skin sample cultivated in 5 % CO_2 at 37 °C until fibroblast outgrowth was sufficient for a transfer to a T25 cell culture flask, in which the cells were cultured in DMEM without Ciprofloxacin and used for further experiments.

2.4.2. Culturing of immortalized human keratinocytes (HaCaT)

Human immortalized keratinocytes (HaCaT) were purchased from Cell Lines Service (Germany) and cultured in standard DMEM medium at 37 °C, 5 % CO_2.

2.5. UV irradiation protocols

2.5.1. UVA1 irradiation of cultured human fibroblasts and immortalized keratinocytes

One day before irradiation, the cells were seeded on a 6-well plate in DMEM without pyruvate at a density of 5×10^4 cells per well and incubated overnight. The decision to maintain the cells in pyruvate-free medium was based on the publication by O'Donnell-Tormey [35], who showed that cells have the ability to self-equilibrate to serum pyruvate levels in about 12 h. This ability makes the 0 mM pyruvate initial culture medium closer to the physiological levels of pyruvate in the body than the widely used 1 mM DMEM medium.

At the beginning of irradiation, the medium was aspirated from each well. Cells were irradiated in 1 mL PBS. For a graphical representation of the irradiation protocol, see Supplementary Figure S1 a. Thedose of UVA1 per single irradiation was provided by a Sellamed-Lamp (Sellas Medizinische Geräte GmbH, Germany) with an emission spectrum of 340–420 nm (s ee Supplementary Figure S1 a) set at 6 J/cm^2. The PBS was then aspirated, and 5 mL fresh medium with 0 mM pyruvate was added to the corresponding wells after the first irradiation. Prior to all subsequent irradiation procedures, the medium was aspirated and collected in separate falcons and then returned to the corresponding wells.

A total of 3 irradiations per day were performed, with a 4 h rest period between each irradiation and an overnight rest period after the last daily irradiation. The whole treatment lasted four days.

2.5.2. UVB irradiation of cultured human fibroblasts and immortalized keratinocytes

One day before irradiation, the cells were seeded on a 6-well plate in DMEM without pyruvate (0 mM) at a density of 1×10^5 cells per well and incubated overnight. The decision to maintain the cells in a pyruvate-free medium was based on the publication by O'Donnell-Tormey [35] (see UVA1 irradiation).

At the beginning of the irradiation, the medium was aspirated from each well. Cells were irradiated in 1 mL PBS. For graphical representation of the irradiation protocol, see Supplementary Figure S1 b. The dose of UVB per single irradiation was provided by a UV Crosslinker (Vilber Lourmat, France) set at 10 mJ/cm^2. The PBS was then aspirated, and 5 mL fresh medium with 0 mM pyruvate was added to the corresponding wells after the first irradiation. Prior to all subsequent irradiation procedures, the medium was aspirated and collected in separate falcons and then returned to the corresponding wells.

A total of 2 irradiations per day were performed, with a 4 h rest period between each irradiation and an overnight rest period after the last daily irradiation. The whole treatment lasted three days.

2.6. RNA extraction from cultured cells and subsequent qPCR analysis of MMP28 expression

RNA was extracted from the treated cells using the NucleoSpin RNA-isolation kit (Machery-Nagel, Germany) according to the manufacturer's protocol. For reverse transcription, 500 ng RNA per sample was used. A master mix was prepared for reverse transcription, containing 1 µL random primer (Roche, Germany), 4 µL 5x buffer (SuperScript II, Invitrogen/Thermo Fisher, Germany), 1 µL dNTPs (New England Bio Labs, Germany), 1 µL DTT (SuperScript II, Invitrogen/Thermo Fisher, Germany), and 2 µL water per sample. Up to 10 µl RNA was added to the mix, and the rest of the volume up to 19 µl was filled with water. The RNA was stretched at 70 °C for 10 min. Afterward, 1 µL SuperScript enzyme (SuperScript II, Invitrogen/Thermo Fisher, Germany) was added to each sample at room temperature followed by incubation at 42 °C for 45 min and subsequently at 70 °C for 10 min. At the end of reverse transcription, the samples were cooled and stored at 4 °C.

For qPCR analysis, each sample contained 10 µL SybrGreen (Roche, Germany), 0.5 µL forward primer, 0.5 µL reverse primer, 8 µL water, and 1 µL cDNA. For negative control, 1 µL of water was used instead of cDNA. 20 µL of each sample were pipetted in duplicates on a 96-well LightCycler plate (Roche, Germany). Optimal annealing temperatures were determined for each gene of interest as shown in Table 3 qPCR reaction was performed in Roche LightCycler 96 (Roche, Germany), programmed for 45 cycles of amplification.

The results were evaluated with LightCycler 96 software, and the MMP28 expression was calculated as a ratio to the housekeeper (b-actin). For subsequent evaluation, MMP28 expression was presented as fold change compared to control (treated with 0J/cm^2 UVA1 and cultured in 1 mM pyruvate).

2.7. Statistical analysis

Prior to the study initiation we determined an effect size between 0.8 and 1.2 to be suitable for calculating our minimal group size in accordance with the publications of Sullivan and Feinn from 2012 [36], Sawilowsky 2009 [37], and Cohen 1988/2013 [38]. Using G*Power 3.1.9.7 (Heinrich-Heine-Universty Dusseldorf, Dermany), we calculated the minimal group size for a one-way ANOVA at alpha error 0.05 and power of 0.8 to be 3 probands.

Statistical analysis was performed with GraphPad Prism 9.5.1 (Graphpad Software Inc, USA). A One-Way ANOVA test was used, and results were considered significant at a p-value <0.05.

Ethical approval

All experiments were approved by the Institutional Review Board of the University of Regensburg, Germany (Permit Number: 22-2890-101). The collection and propagation of primary human fibroblasts was

Table 3
Product size and annealing temperatures of the used primers (Sigma-Aldrich, Germany).

Gene of interest	Primer sequence: forward/reverse	Size of product (bp–base pairs)	Annealing temperature
MMP28	GTGCAGAGCCTGTATGGGAA/ TGCCTGTCTACAGTGATGGC	172	60 °C
b-Actin	CTACGTCGCCCTGGACTTCGAGC/ GATGGAGCCGCCGATCCACACGG	385 bp	54–65 °C

approved by the Institutional Review Board of the University of Regensburg (Permit Number: 14101 0001).

7. Results

7.1. Lupus erythematosus and healthy skin showed differences in the expression patterns of MMP1 and MMP28

We analyzed the expression patterns of MMP1 and MMP28 (Fig. 1). Most CLE subtypes, as well as SLE and PLE, showed a statistically significant upregulation of MMP1 expression compared to HS. MMP1 levels in Chilblain LE and ACLE were elevated but not statistically significant compared to HS (Fig. 1a). MMP1 was mainly detected in the cytoplasm, but there was also sporadic nuclear staining independent of the LE subtype (Supplementary Fig. S2).

Compared to MMP1, MMP28 showed no difference in expression intensity between LE and HS. However, MMP28 showed a very distinct vertical distribution pattern. Of the LE and PLE samples assessed, Chilblain LE showed a broad distribution of MMP28 with scoring values of 3–4, reaching as deep as the *S. basale* and dermis (Fig. 1b and c). In contrast, all other LE subtypes and the HS samples showed mostly moderate spread of MMP28 in the upper layers of the epidermis without involvement of the *S. basale* (Fig. 1b and c). Exceptions were the samples from patients with PLE, where three out of five patients showed MMP28 expression similar to that seen in Chilblain LE. Interestingly, in cases in which MMP28 was exclusively expressed in the epidermis, the staining was cytoplasmatic (Fig. 1 c LET, SCLE, DLE, SLE, ACLE, and NS). However, samples showing *S. basale* and dermal staining showed nuclear MMP28 expression in these two regions (Fig. 1 c Chilblain and PLE).

Overall, the histological analysis of MMP1 and MMP28 expression revealed increased MMP1 levels in LE. Furthermore, a distinct vertical distribution of MMP28 in Chilblain LE and PLE was observed.

7.2. UVA1 and UVB had different effects on MMP28 expression in cultured fibroblasts and keratinocytes

Our group and others have shown that UVA1 and UVB irradiation influence the expression of MMP1 [39–41]. However, the influence of UVR on MMP28 expression has been studied in less detail.

Although MMP28 expression has been described mainly in keratinocytes [15,17,18], we observed sporadic nuclear staining in *S. basale* adjacent dermal fibroblasts (Fig. 1 c). Therefore, we applied repetitive low doses of UVA1 and UVB on both primary fibroblasts (Re5) and immortalized keratinocytes (HaCaT) (for irradiation protocol see Supplementary Figure S. 1).

In HaCaT cells, UVB had no influence on MMP28 expression. MMP28 levels in Re5 fibroblasts were increased after UVB treatment compared to untreated controls, but the increase was not statistically significant (Fig. 2 a).

Similar to UVB, UVA1 had no significant effect on MMP28 expression in HaCaT cells, despite a slight increase in mRNA levels compared to the control samples (Fig. 2 b). In fibroblast samples, however, UVA1 irradiation significantly increased MMP28 expression compared to

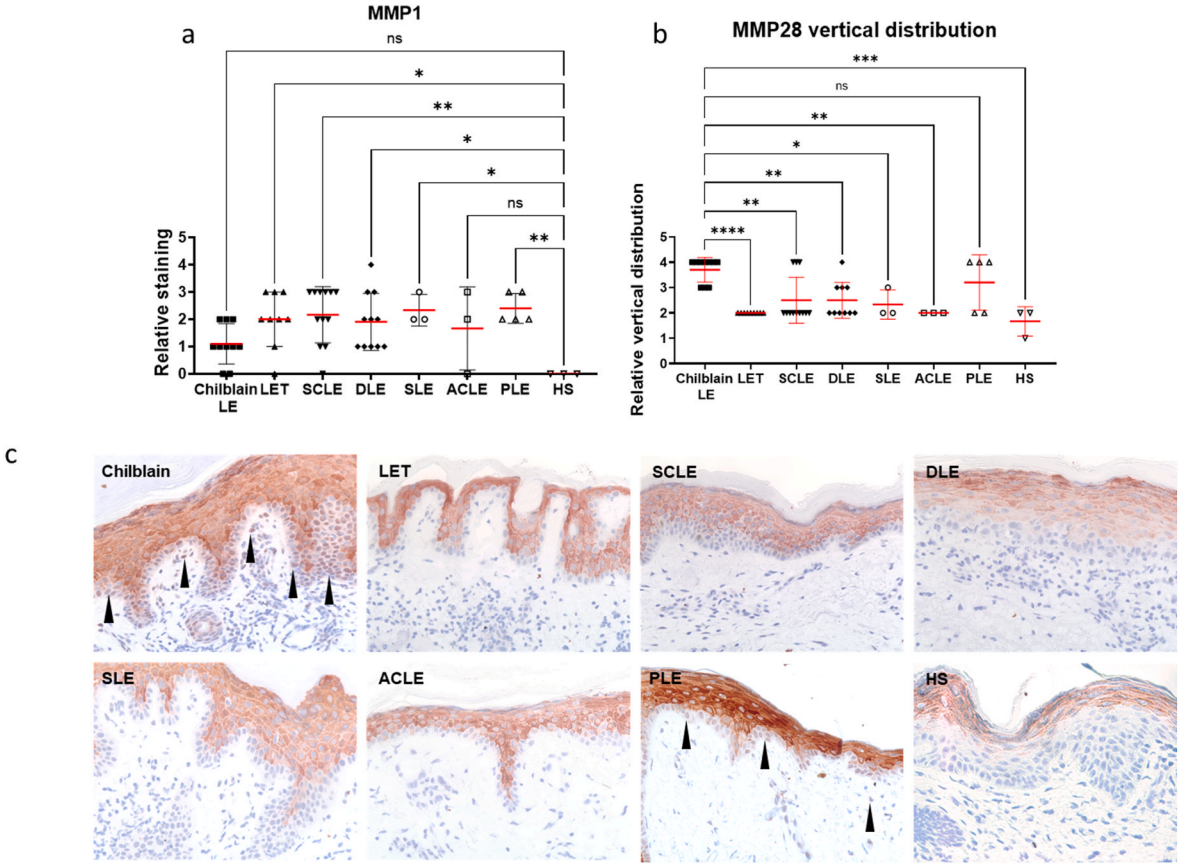

Fig. 1. Histological analysis of MMP1 and MMP28 reveals an increased MMP1 levels in LE and distinct vertical distribution of MMP28 in Chilblain LE and PLE. (a) Most CLE subtypes, as well as SLE and PLE, show a statistically significant upregulation of MMP1 expression when compared to healthy skin. Chilblain LE and ACLE show a not-significant increase in MMP1 expression compared to healthy skin (HS). (b) Chilblain LE and PLE show the deepest vertical distribution of MMP28 compared to the other CLE sub-types, SLE, and healthy skin. (c) Representative histologic staining shows the vertical distribution of MMP28. Black arrowheads show MMP28 expression in the dermis. Statistical analysis: One-way ANOVA with Dunnett's multiple comparisons test; for significances: (ns) $P > 0.05$; (*) $P < 0.05$; (**) $P < 0.01$; (***) $P < 0.001$; (****) $P < 0.0001$).

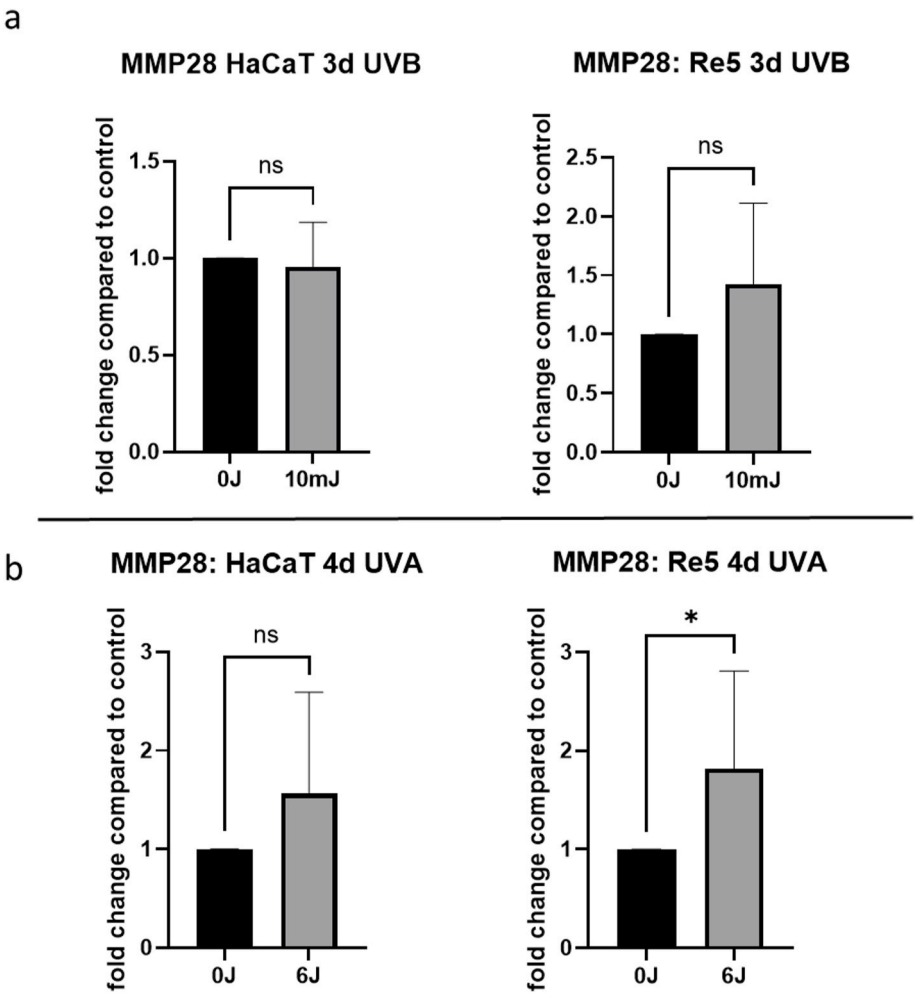

Fig. 2. UV irradiation increases the expression of MMP28 in primary fibroblasts *in vitro*. (a) MMP28 expression measured in HaCaT and Re5 cells after UVB irradiation. Although Re5 showed a tendency to increase MMP28, no significant expression of upregulation was observed after irradiation. (b) MMP28 expression measured in HaCaT and Re5 cells after UVA1 irradiation. No significant differences in expression in HaCaT cells after treatment. Re5 cells show a significant increase in MMP28 expression after UVA1 irradiation. Statistical analysis: Student's t-test; for significances: (ns) $P > 0.05$; (*) $P < 0.05$).

untreated controls (Fig. 2 b).

In conclusion, UVA had stronger influence on MMP28 up-regulation than UVB, especially in primary fibroblasts.

7.3. Inverse correlation between MMP28 and GLUT1 expression in the epidermis

MMP28 has shown a UVA1-dependent expression pattern in fibroblasts (Fig. 2). However, we have previously shown that UVA1 irradiation not only modulates MMP expression but also affects the cell metabolism, in particular by increasing glucose metabolism [39]. Because of literature reports that glucose is a bona fide modulator of MMP expression [42,43], we wanted to see whether the distinct vertical distribution of MMP28 observed by immunohistochemistry (Fig. 1) correlates with the expression of the glucose transporter GLUT1 (Fig. 3 and Supplementary Fig. S2).

As shown in Fig. 3 a, Chilblain LE had the lowest epidermal expression of GLUT1 compared to HS, followed by PLE. All remaining LE subtypes had GLUT1 levels higher than that of HS. In contrast, the GLUT1 expression in the dermis of all LE patients was higher than that in the dermis of healthy people (Fig. 3 b). PLE patients showed slightly reduced dermal expression of GLUT1 (Fig. 3 b).

A correlation was found between the expression levels of GLUT1 and the vertical distribution of MMP28 (Fig. 3 c). The lower GLUT1 levels in the epidermis observed in Chilblain LE and PLE resulted in increased vertical distribution of MMP28. The remaining LE subtypes with high levels of epidermal GLUT1 had a flatter MMP28 distribution. In HS, GLUT1 and MMP28 levels were uniformly low and did not show the inverse correlation observed in the LE samples.

In summary, GLUT1 levels in the dermis of all LE patients were elevated compared to HS. In the epidermis, GLUT1 expression and MMP28 vertical distribution showed an inverse correlation.

7.4. Inverse correlation between miR-31/miR-150 and GLUT1 expression in the epidermis

Glucose uptake can be regulated by miR-31 and miR-150 via the GLUT1 receptor [27,30,44]. Furthermore, these two micro RNAs are also differentially expressed in patients with SLE [24,25,45]. We therefore investigated the expression of miR-31 and miR-150 in relation to GLUT1 in our study cohort using *in situ* hybridization and immunohistochemistry (Fig. 4).

Most LE subtypes showed levels of miR-31 expression similar to those observed in HS (Fig. 4 a). Only Chilblain LE showed a statistically significant increase in miR-31 expression, up to 100-fold compared to other LE subtypes. In the case of miR-150 (Fig. 4 b), Chilblain LE again showed the highest expression of all LE subtypes. Furthermore, only Chilblain LE had significantly higher miR-150 levels than HS controls.

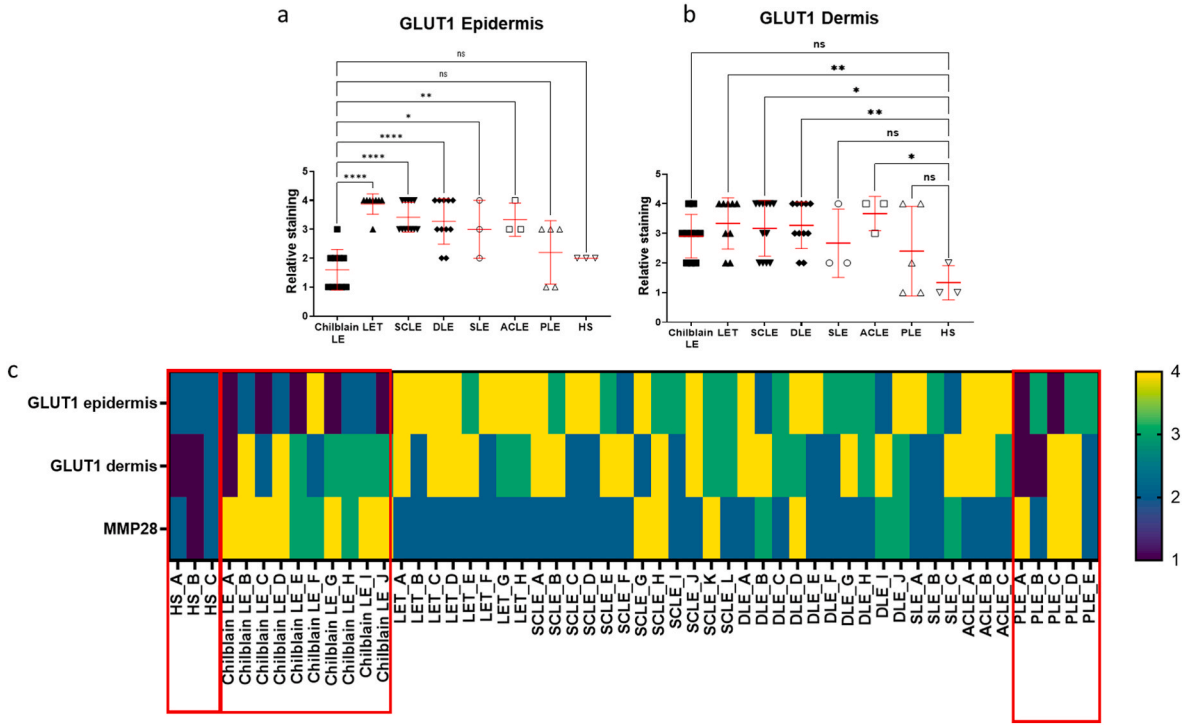

Fig. 3. Histological analysis reveals an inverse correlation of the expression patterns of epidermal GLUT1 and MMP28 in LE patients. (a) Chilblain LE shows the lowest epidermal expression of GLUT1 of all CLE sub-types. (b) All CLE sub-types and SLE show increased levels of GLUT1 in the dermis when compared to healthy skin. (c) Heat-map matching the vertical distribution of MMP28 to the expression patterns of GLUT1 in the epidermis and dermis. There is an inverse correlation between the GLUT1 levels in the dermis and the spread of MMP28 into the dermis. Statistical analysis: One-way ANOVA with Dunnett's multiple comparisons test; for significances: (ns) $P > 0.05$; (*) $P < 0.05$; (**) $P < 0.01$; (****) $P < 0.0001$).

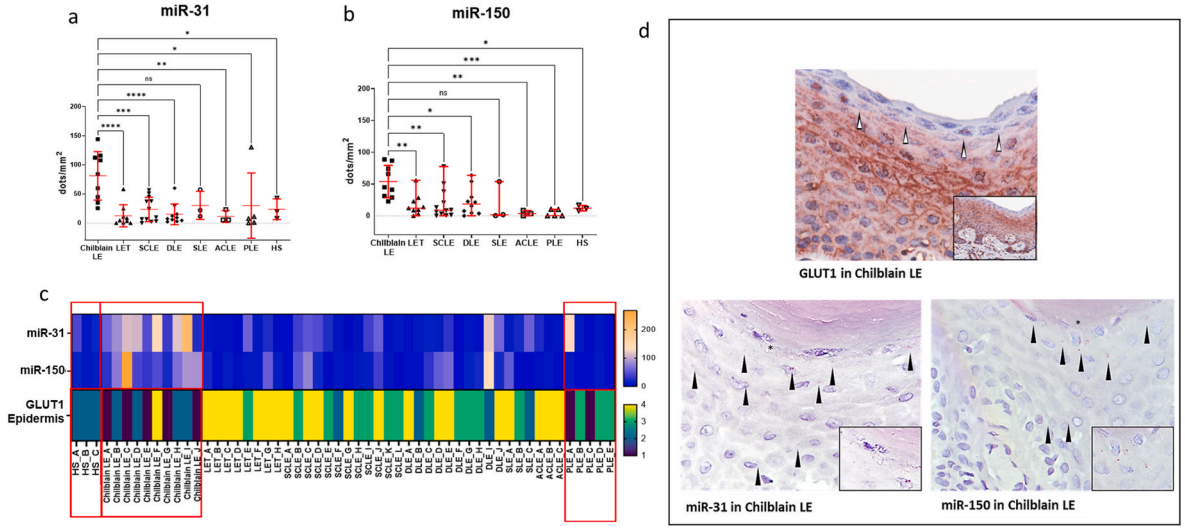

Fig. 4. Histological analysis reveals an inverse correlation of the expression patterns of miR-31, miR-150, and GLUT1 in the epidermis of LE patients. (a) Chilblain LE shows the highest expression of miR-31 of all CLE sub-types, SLE, PLE, and healthy skin. (b) Chilblain LE shows the highest expression of miR-150 of all CLE sub-types, SLE, PLE, and healthy skin. (c) Heat-map matching the expression of miR-31 and miR-150 to the expression of GLUT1 in the epidermis. There is an inverse correlation between miR-31/150 expression and the levels of GLUT1 in the epidermis, especially in Chilblain LE and PLE. (d) Representative histological images showing the distribution of GLUT1 (40x magnification, small image 20x overview) and miR-31/150 (60x magnification, asterisk corresponds with the zoomed-in area depicted in the small image(s)). Black arrowheads show the miR distribution. White arrowheads point at the area in the GLUT1 staining that correlates with the highest miR-31/150 expression. GLUT1 decreased in areas with a high prevalence of miR-31/150. Statistical analysis: One-way ANOVA with Dunnett's multiple comparisons test; for significances: (ns) $P > 0.05$; (*) $P < 0.05$; (**) $P < 0.01$; (***) $P < 0.001$; (****) $P < 0.0001$).

For both miR-31 and miR-150, expression was detected only in the epidermis of the tested samples, but not in the dermis.

We subsequently compared the *in situ* hybridization data for miR-31 and miR-150 with the expression of the GLUT1 glucose transporter in the epidermis (Fig. 4 c). HS had overall low levels of miR-31, miR-150, and GLUT1. The results for Chilblain LE differed again from all remaining LE subtypes. While the majority of LE had low levels of miR-31 and miR-150, similar to HS, which correlates with low GLUT1

expression, Chilblain had low epidermal values for GLUT1 and high expression of miR-31 and miR-150.

The inverse correlation between the expression of GLUT1, miR-31, and miR-150 observed in the LE samples was also detected histologically (Fig. 4 d). Interestingly, PLE samples, which previously showed an MMP28 and GLUT1 correlation similar to that in Chilblain LE (Fig. 3 c), had low levels of epidermal GLUT1 that did not coincide with a notable increase in miR-31 or miR-150.

Overall, Chilblain LE had the highest expression of miR-31 and miR-150 of all LE subtypes. The expression patterns of both miR-31 and miR-150 inversely correlated with the GLUT1 levels observed in the epidermis.

8. Discussion

Exposure to the sun, and UVR in particular, can trigger a wide range of processes in the skin, negatively affecting tissue homeostasis. Major contributors to the structural remodeling of the skin are MMPs.

As shown in this and other studies [6,39,46], UV exposure can increase MMP expression even in HS, specifically in fibroblasts and keratinocytes. As such, it is an important finding that the samples taken from UV-induced lesions in patients with LE and PLE showed a significant increase in MMP1 compared to HS controls, which were also taken from light-exposed areas. Interestingly, Chilblain LE showed the lowest MMP1 expression of the LE subtypes investigated, although the finding was not statistically significant. An increase in MMP1 expression may indicate active tissue rearrangement and aberrant immune cell migration as observed in LE lesions [47,48]. The sporadic nuclear localization of the marker, observed mainly in LE and PLE samples, could be an indication of the initialization of a skin cell survival mechanism after UVR since nuclear MMP1 has been reported to have an anti-apoptotic function [49]. However, sun-exposed HS samples showed almost no MMP1 staining and no nuclear localization of the marker. The absence of nuclear MMP1 in HS compared to LE and PLE casts doubt on the anti-apoptotic function of MMP1 in these photosensitive diseases, especially since keratinocyte apoptosis is the major factor for LE initiation, development, and perpetuation [48]. Further studies are needed to clarify the function of MMP1 in LE.

In the case of MMP28, the most prominent difference between LE, PLE, and HS was the spatial distribution of MMP28, not only in the form of the vertical distribution depth in the tissue but also in the sub-cellular distribution of the marker. Of all samples tested, Chilblain LE and PLE samples had the deepest vertical distribution of MMP28, coupled with nuclear localization of the marker in the *S. basale* of the epidermis and in cells in proximity to the papillary dermis. No explanation has yet been found for this distribution pattern, as these two diseases differ significantly in their pathogenesis. This finding will be investigated in upcoming studies. As far as we know, this is the first time that nuclear localization and dermal distribution of MMP28 have been observed in the skin of patients with LE. Nuclear expression of MMP28 has been previously described in pulmonary fibrosis [50] and during wound healing [15], consistent with its ascribed functions as a driver of cell proliferation and epithelial-to-mesenchymal transition. These functions may correlate closely with the clinical manifestations of Chilblain LE including plaque-like infiltrates and fissural hyperkeratosis accompanied by small ulcerations [51]. In addition, the fact that Chilblain LE had low MMP1 expression in contrast to significantly elevated MMP28 levels compared to all other LE subtypes could be an indication of a designated disease-specific function of MMP28. Further studies are needed to determine whether MMP28 could serve as a supporting diagnostic marker for Chilblain LE.

Considering the histologic detection of MMP28 in fibroblasts and bearing in mind the role of UVR as a trigger for LE, we wanted to test its influence on cultured fibroblasts and keratinocytes. UVB and short-wave UVA2 (320–340 nm) are known to promote LE flare-ups [52], while low doses of long-wave UVA1 (340–400 nm) have shown beneficial effects in patients with LE [52,53]. Taking into consideration the dual effect of UVR to either exacerbate or alleviate LE effects, we chose to use both UVB and UVA1 sources in our *in vitro* experiments. The increase in MMP28 transcription after UVA1 irradiation matched the immunohistochemistry findings. Compared to UVB, UVA1 can penetrate deeper into the skin, reaching the dermis and resident fibroblasts [54,55]. According to the current literature, this is the first time that UVA1-mediated regulation has been described for MMP28 in fibroblasts.

Knowing that UVA1 irradiation modulates both MMPs and skin glucose metabolism [39] and considering the function of glucose as a bona fide modulator of MMP expression [42,43], we investigated a possible connection between MMP28 expression patterns and the dysregulation of glucose metabolism in LE and PLE samples. Indications of a higher prevalence of metabolic syndrome, which includes elevated fasting glucose levels, have been observed for patients with SLE and Lupus nephritis [56,57]. However, since other organs such as the heart and kidneys were the focus points of those studies, little is known about the metabolic balance in the skin of LE patients. As such, a possible correlation between tissue remodeling, in the form of MMP28 expression, and skin metabolism, in the form of GLUT1 expression, is important in the context of LE. GLUT1 is one of the major glucose transporters, and its upregulation correlates with increased glucose uptake [58].

We have shown that all LE subtypes and PLE have increased GLUT1 levels in the dermis compared to HS. In the epidermis, Chilblain LE and PLE had low GLUT1 expression while the other LE subtypes showed elevated GLUT1 levels compared to HS. These findings indicate potential metabolic aberrations in the skin of LE patients. The observed distinct compartmentalization of glucose transporters in the skin layers between different photosensitive diseases and disease sub-types may indicate different functions of glucose in the context of LE. Still, further and more precise studies are needed to examine the metabolic fingerprint of the skin between different LE subtypes.

We further observed an inverse correlation between GLUT1 expression levels in the epidermis and MMP28 distribution depth in LE and PLE compared to HS. Considering that GLUT1 overexpression corresponds to increased glucose uptake [58], the observed inverse correlation between GLUT1 and MMP28 may represent a novel glucose-regulated pathway of MMP28 expression. Such metabolic regulation of MMP28 is in accordance with the already published scientific data, showing that glucose concentrations not only upregulate [43] but also downregulate [42] MMPs.

Since miR-31 and miR-150 are established aberrant markers in LE [25,59] and can also regulate GLUT1 expression [27,30], we compared the epidermal expression of these two miRs with the data on GLUT1. Chilblain LE showed the highest expression of miR-31 and miR-150 of all LE subtypes. In most Chilblain LE samples as well as PLE, miR-31 and miR-150 levels did not increase above those found in HS. Usually, high levels of miR-31 and miR-150 correspond to low levels of GLUT1 as shown by Wan et al. and Yuan et al. [27,30]. It is possible that miR-regulated GLUT1 expression is a predominant characteristic of LE with PLE skin regulating glucose uptake by other mechanisms, considering that PLE samples showed low levels of GLUT1 but almost no miR-31 or miR-150 expression.

In summary, the novel MMP28 expression pattern we describe and its inverse correlation with GLUT1 expression in the epidermis present new opportunities in LE diagnostic and treatment. However, further studies are needed to confirm MMP28 as an additional diagnostic marker for Chilblain LE and PLE. Larger patient cohorts will be necessary to validate its robustness and suitability for clinical application.

Additionally, further *in vitro* and *in vivo* experiments are essential to explore the metabolic component of MMP28 regulation and its role in UV-induced skin or systemic symptoms in LE patients. Analysis of the glucose flux as well as enzyme and transporter activity need to be conducted on top of histological assays in order to elaborate and reinforce the data presented in this work. Such studies would expand on the simple correlation between MMP28 and GLUT1 established in the

current paper, investigating a causal link between those markers and LE symptoms – an essential step for developing new LE treatments.

Nevertheless, we believe the data presented in this study provides a strong foundation for future advancements in LE understanding and treatment.

9. Conclusion

We have shown a novel MMP28 expression pattern in Chilblain LE and PLE and a UVA1-dependent regulation of MMP28 in human fibroblasts for the first time. Furthermore, our results suggest a metabolic component of MMP28 regulation with a glucose-dependent mechanism.

CRediT authorship contribution statement

I. Ivanova: Writing – review & editing, Writing – original draft, Visualization, Validation, Methodology, Investigation, Formal analysis, Data curation, Conceptualization. **T. Svilenska:** Writing – review & editing. **T. Maisch:** Writing – review & editing. **S. Karrer:** Writing – review & editing, Supervision, Formal analysis. **D. Niebel:** Writing – review & editing. **M. Berneburg:** Writing – review & editing, Investigation, Formal analysis. **B. Kurz:** Writing – review & editing, Writing – original draft, Validation, Supervision, Resources, Investigation, Formal analysis, Data curation.

Ethics statement

This study was approved by the Ethics Committee of the University of Regensburg, Germany (Permit Number: 22-2890-101).

Funding sources

The authors did not receive any funding for this work.

Declaration of competing interest

The authors declare that they have no known competing financial interests or personal relationships that could have appeared to influence the work reported in this paper.

Acknowledgements

The authors thank Monika Schöll for the linguistic revision of the manuscript.

Appendix A. Supplementary data

Supplementary data to this article can be found online at https://doi.org/10.1016/j.jtauto.2024.100265.

Data availability

Data will be made available on request.

References

[1] F. Rees, M. Doherty, M.J. Grainge, P. Lanyon, W. Zhang, The worldwide incidence and prevalence of systemic lupus erythematosus: a systematic review of epidemiological studies, Rheumatology 56 (2017) 1945–1961, https://doi.org/10.1093/rheumatology/kex260.

[2] D. Niebel, L. de Vos, T. Fetter, C. Bragelmann, J. Wenzel, Cutaneous lupus erythematosus: an update on pathogenesis and future therapeutic directions, Am. J. Clin. Dermatol. 24 (2023) 521–540, https://doi.org/10.1007/s40257-023-00774-8.

[3] P. Avar-Aydın, H.I. Brunner, Revisiting childhood-onset systemic lupus erythematosus, Turk Arch Pediatr 59 (2024) 336–344, https://doi.org/10.5152/TurkArchPediatr.2024.24097.

[4] M.C. Hochberg, Updating the American College of Rheumatology revised criteria for the classification of systemic lupus erythematosus, Arthritis Rheum.: Official Journal of the American College of Rheumatology 40 (1997), https://doi.org/10.1002/art.1780400928, 1725-1725.

[5] M. Petri, A.-M. Orbai, G.S. Alarcón, C. Gordon, J.T. Merrill, P.R. Fortin, I.N. Bruce, D. Isenberg, D.J. Wallace, O. Nived, G. Sturfelt, R. Ramsey-Goldman, S.-C. Bae, J. G. Hanly, J. Sánchez-Guerrero, A. Clarke, C. Aranow, S. Manzi, M. Urowitz, D. Gladman, K. Kalunian, M. Costner, V.P. Werth, A. Zoma, S. Bernatsky, G. Ruiz-Irastorza, M.A. Khamashta, S. Jacobsen, J.P. Buyon, P. Maddison, M.A. Dooley, R. F. van Vollenhoven, E. Ginzler, T. Stoll, C. Peschken, J.L. Jorizzo, J.P. Callen, S. S. Lim, B.J. Fessler, M. Inanc, D.L. Kamen, A. Rahman, K. Steinsson, A.G. Franks Jr., L. Sigler, S. Hameed, H. Fang, N. Pham, R. Brey, M.H. Weisman, G. McGwin Jr., L. S. Magder, Derivation and validation of the Systemic Lupus International Collaborating Clinics classification criteria for systemic lupus erythematosus, Arthritis Rheum. 64 (2012) 2677–2686, https://doi.org/10.1002/art.34473.

[6] P. Pittayapruek, J. Meephansan, O. Prapapan, M. Komine, M. Ohtsuki, Role of matrix metalloproteinases in photoaging and photocarcinogenesis, Int. J. Mol. Sci. 17 (2016) 868, https://doi.org/10.3390/ijms17060868.

[7] A. O'Grady, C. Dunne, P. O'Kelly, G. Murphy, M. Leader, E. Kay, Differential expression of matrix metalloproteinase (MMP)-2, MMP-9 and tissue inhibitor of metalloproteinase (TIMP)-1 and TIMP-2 in non-melanoma skin cancer: implications for tumour progression, Histopathology 51 (2007) 793–804, https://doi.org/10.1111/j.1365-2559.2007.02885.x.

[8] T. Itoh, H. Matsuda, M. Tanioka, K. Kuwabara, S. Itohara, R. Suzuki, The role of matrix metalloproteinase-2 and matrix metalloproteinase-9 in antibody-induced arthritis, J. Immunol. 169 (2002) 2643–2647, https://doi.org/10.4049/jimmunol.169.5.2643.

[9] H. Ainiala, A. Hietaharju, P. Dastidar, J. Loukkola, T. Lehtimäki, J. Peltola, M. Korpela, T. Heinonen, S.T. Nikkari, Increased serum matrix metalloproteinase 9 levels in systemic lupus erythematosus patients with neuropsychiatric manifestations and brain magnetic resonance imaging abnormalities, Arthritis Rheum. 50 (2004) 858–865, https://doi.org/10.1002/art.20045.

[10] Y.-H. Chang, I.-L. Lin, G.J. Tsay, S.-C. Yang, T.-P. Yang, K.-T. Ho, T.-C. Hsu, M.-Y. Shiau, Elevated circulatory MMP-2 and MMP-9 levels and activities in patients with rheumatoid arthritis and systemic lupus erythematosus, Clin. Biochem. 41 (2008) 955–959, https://doi.org/10.1016/j.clinbiochem.2008.04.012.

[11] A. Faber-Elmann, Z. Sthoeger, A. Tcherniack, M. Dayan, E. Mozes, Activity of matrix metalloproteinase-9 is elevated in sera of patients with systemic lupus erythematosus, Clin. Exp. Immunol. 127 (2002) 393–398, https://doi.org/10.1046/j.1365-2249.2002.01758.x.

[12] G. Keyszer, I. Lambiri, R. Nagel, C. Keysser, M. Keysser, E. Gromnica-Ihle, J. Franz, G. Burmester, K. Jung, Circulating levels of matrix metalloproteinases MMP-3 and MMP-1, tissue inhibitor of metalloproteinases 1 (TIMP-1), and MMP-1/TIMP-1 complex in rheumatic disease. Correlation with clinical activity of rheumatoid arthritis versus other surrogate markers, J. Rheumatol. 26 (1999) 251–258. http://www.ncbi.nlm.nih.gov/pubmed/9972954.

[13] C. Mawrin, A. Brunn, C. Röcken, J.M. Schröder, Peripheral neuropathy in systemic lupus erythematosus: pathomorphological features and distribution pattern of matrix metalloproteinases, Acta Neuropathol. 105 (2003) 365–372, https://doi.org/10.1007/s00401-002-0653-2.

[14] G. Ertugrul, D. Keles, G. Oktay, S. Aktan, Matrix metalloproteinase-2 and -9 activity levels increase in cutaneous lupus erythematosus lesions and correlate with disease severity, Arch. Dermatol. Res. 310 (2018) 173–179, https://doi.org/10.1007/s00403-018-1811-2.

[15] U. Saarialho-Kere, E. Kerkelä, S. Suomela, T. Jahkola, J. Keski-Oja, J. Lohi, Epilysin (MMP-28) expression is associated with cell proliferation during epithelial repair, J. Invest. Dermatol. 119 (2002) 14–21, https://doi.org/10.1046/j.1523-1747.2002.01790.x.

[16] A. Kuhn, M. Herrmann, S. Kleber, M. Beckmann-Welle, K. Fehsel, A. Martin-Villalba, P. Lehmann, T. Ruzicka, P.H. Krammer, V. Kolb-Bachofen, Accumulation of apoptotic cells in the epidermis of patients with cutaneous lupus erythematosus after ultraviolet irradiation, Arthritis Rheum. 54 (2006) 939–950, https://doi.org/10.1002/art.21658.

[17] S.A. Illman, J. Lohi, J. Keski-Oja, Epilysin (MMP-28) – structure, expression and potential functions, Exp. Dermatol. 17 (2008) 897–907, https://doi.org/10.1111/j.1600-0625.2008.00782.x.

[18] J. Lohi, C.L. Wilson, J.D. Roby, W.C. Parks, Epilysin, a novel human matrix metalloproteinase (MMP-28) expressed in testis and keratinocytes and in response to injury, J. Biol. Chem. 276 (2001) 10134–10144, https://doi.org/10.1074/jbc.M001599200.

[19] A. Kraemer, I.P. Chen, S. Henning, A. Faust, B. Volkmer, M.J. Atkinson, S. Moertl, R. Greinert, UVA and UVB irradiation differentially regulate microRNA expression in human primary keratinocytes, PLoS One 8 (2014) e83392, https://doi.org/10.1371/journal.pone.0083392.

[20] Y. Tu, W. Wu, Y. Guo, F. Lu, D. Xu, X. Li, Y. Zhao, L. He, Upregulation of hsa-miR-31-3p induced by ultraviolet affects keratinocytes permeability barrier by targeting CLDN1, Biochem. Biophys. Res. Commun. 532 (2020) 626–632, https://doi.org/10.1016/j.bbrc.2020.06.113.

[21] S. Quinodoz, M. Guttman, Long noncoding RNAs: an emerging link between gene regulation and nuclear organization, Trends Cell Biol. 24 (2014) 651–663, https://doi.org/10.1016/j.tcb.2014.08.009.

[22] D. Cretoiu, J. Xu, J. Xiao, S.M. Cretoiu, Telocytes and their extracellular vesicles—evidence and Hypotheses, Int. J. Mol. Sci. 17 (2016) 1322, https://doi.org/10.3390/ijms17081322.

[23] A.M. Ardekani, M.M. Naeini, The role of MicroRNAs in human diseases, Avicenna J. Med. Biotechnol. (AJMB) 2 (2010) 161–179. https://www.ncbi.nlm.nih.gov/pmc/articles/PMC3558168. https://pubmed.ncbi.nlm.nih.gov/23407304.

[24] W. Fan, D. Liang, Y. Tang, B. Qu, H. Cui, X. Luo, X. Huang, S. Chen, B.W. Higgs, B. Jallal, Y. Yao, J.B. Harley, N. Shen, Identification of microRNA-31 as a novel regulator contributing to impaired interleukin-2 production in T cells from patients with systemic lupus erythematosus, Arthritis Rheum. 64 (2012) 3715–3725, https://doi.org/10.1002/art.34596.
[25] C. Solé, S. Domingo, B. Ferrer, T. Moliné, J. Ordi-Ros, J. Cortés-Hernández, MicroRNA expression profiling identifies miR-31 and miR-485-3p as regulators in the pathogenesis of discoid cutaneous lupus, J. Invest. Dermatol. 139 (2019) 51–61, https://doi.org/10.1016/j.jid.2018.07.026.
[26] M.T. Fernández-Figueras, C. Carrato, X. Saenz-Sardà, E. Musulén, M.J. Fuente, L. Puig, MicroRNA31 and MMP-1 contribute to the differentiated pathway of invasion -with enhanced epithelial-to-mesenchymal transition- in squamous cell carcinoma of the skin, Arch. Dermatol. Res. 314 (2022) 767–775, https://doi.org/10.1007/s00403-021-02288-x.
[27] M.-J. Wang, H.-J. Huang, Y.-Y. Xu, H. Vos, C. Gulersonmez, E. Stigter, J. Gerritsen, M.P. Gallego, R. van Es, L. Li, H. Deng, L. Han, R.-Y. Huang, C.-J. Lu, B. M. Burgering, Metabolic rewiring in keratinocytes by miR-31-5p identifies therapeutic intervention for psoriasis, EMBO Mol. Med. 15 (2023) e15674, https://doi.org/10.15252/emmm.202215674.
[28] X. Zhao, R. Dong, Z. Tang, J. Wang, C. Wang, Z. Song, B. Ni, L. Zhang, X. He, Y. You, Circular RNA circLOC101928570 suppresses systemic lupus erythematosus progression by targeting the miR-150-5p/c-myb axis, J. Transl. Med. 20 (2022) 547, https://doi.org/10.1186/s12967-022-03748-2.
[29] S. Méndez-Flores, J. Furuzawa-Carballeda, G. Hernández-Molina, G. Ramírez-Martinez, N.E. Regino-Zamarripa, B. Ortiz-Quintero, L. Jiménez-Alvarez, A. Cruz-Lagunas, J. Zúñiga, MicroRNA expression in cutaneous lupus: a new window to understand its pathogenesis, Mediators Inflamm 2019 (2019) 5049245, https://doi.org/10.1155/2019/5049245.
[30] G. Yuan, Y. Zhao, D. Wu, C. Gao, Mir-150 up-regulates Glut1 and increases glycolysis in osteosarcoma cells, Asian Pac. J. Cancer Prev. 18 (2017) 1127–1131, https://doi.org/10.22034/apjcp.2017.18.4.1127.
[31] R. Curiel, E.A. Akin, G. Beaulieu, L. DePalma, M. Hashefi, PET/CT imaging in systemic lupus erythematosus, Ann. N. Y. Acad. Sci. 1228 (2011) 71–80, https://doi.org/10.1111/j.1749-6632.2011.06076.x.
[32] E. Zezina, O. Sercan-Alp, M. Herrmann, N. Biesemann, Glucose transporter 1 in rheumatoid arthritis and autoimmunity, Wiley Interdiscip. Rev. Syst. Biol. Med 12 (2020) e1483, https://doi.org/10.1002/wsbm.1483.
[33] N. Fedchenko, J. Reifenrath, Different approaches for interpretation and reporting of immunohistochemistry analysis results in the bone tissue – a review, Diagn. Pathol. 9 (2014) 221, https://doi.org/10.1186/s13000-014-0221-9.
[34] W. Remmele, H.E. Stegner, [Recommendation for uniform definition of an immunoreactive score (IRS) for immunohistochemical estrogen receptor detection (ER-ICA) in breast cancer tissue], Pathologe 8 (1987) 138–140. https://pubmed.ncbi.nlm.nih.gov/3303008/.
[35] J. O'Donnell-Tormey, C.F. Nathan, K. Lanks, C.J. DeBoer, J. de la Harpe, Secretion of pyruvate. An antioxidant defense of mammalian cells, J. Exp. Med. 165 (1987) 500–514, https://doi.org/10.1084/jem.165.2.500.
[36] G.M. Sullivan, R. Feinn, Using effect size-or why the P value is not enough, J. Grad. Med. Educ. 4 (2012) 279–282, https://doi.org/10.4300/jgme-d-12-00156.1.
[37] S.S. Sawilowsky, New effect size rules of thumb, J. Mod. Appl. Stat. Methods 8 (2009) 597–599, https://doi.org/10.22237/jmasm/1257035100.
[38] J. Cohen, Statistical Power Analysis for the Behavioral Sciences, routledge, 2013.
[39] I. Ivanova, C. Bogner, W. Gronwald, M. Kreutz, B. Kurz, T. Maisch, Y. Kamenisch, M. Berneburg, UVA-induced metabolic changes in non-malignant skin cells and the potential role of pyruvate as antioxidant, Photochem. Photobiol. Sci. (2023), https://doi.org/10.1007/s43630-023-00419-z.
[40] B. Catalgol, I. Ziaja, N. Breusing, T. Jung, A. Höhn, B. Alpertunga, P. Schroeder, N. Chondrogianni, E.S. Gonos, I. Petropoulos, B. Friguet, L.-O. Klotz, J. Krutmann, T. Grune, The proteasome is an integral part of solar ultraviolet A radiation-induced gene expression, J. Biol. Chem. 284 (2009) 30076–30086, https://doi.org/10.1074/jbc.M109.044503.
[41] C. Kim, H.C. Ryu, J.H. Kim, Low-dose UVB irradiation stimulates matrix metalloproteinase-1 expression via a BLT2-linked pathway in HaCaT cells, Exp. Mol. Med. 42 (2010) 833–841, https://doi.org/10.3858/emm.2010.42.12.086.
[42] S.V. McLennan, E. Fisher, S.Y. Martell, A.K. Death, P.F. Williams, J.G. Lyons, D. K. Yue, Effects of glucose on matrix metalloproteinase and plasmin activities in mesangial cells: possible role in diabetic nephropathy, Kidney Int. 58 (2000) S81–S87, https://doi.org/10.1046/j.1523-1755.2000.07713.x.
[43] W.-C. Tsai, F.-C. Liang, J.-W. Cheng, L.-P. Lin, S.-C. Chang, H.-H. Chen, J.-H. S. Pang, High glucose concentration up-regulates the expression of matrix metalloproteinase-9 and -13 in tendon cells, BMC Musculoskel. Disord 14 (2013) 255, https://doi.org/10.1186/1471-2474-14-255.
[44] M.-J. Wang, Y.-Y. Xu, H. Vos, C. Gulersonmez, E. Stigter, J. Gerritsen, M.P. Gallego, R. van Es, L. Li, H. Deng, L. Han, R.-Y. Huang, C.-J. Lu, B.M.T. Burgering, Hsa-miR-31-5p controls a metabolic switch in psoriatic keratinocytes that identifies therapeutic intervention, bioRxiv (2022), https://doi.org/10.1101/2022.01.21.477183, 2022.01.21.477183.
[45] M. Nakhjavani, J. Etemadi, T. Pourlak, Z. Mirhosaini, S. Zununi Vahed, S. Abediazar, Plasma levels of miR-21, miR-150, miR-423 in patients with lupus nephritis, Iran, J. Kidney Dis. 13 (2019) 198–206. https://pubmed.ncbi.nlm.nih.gov/31209193/.
[46] I. Ivanova, B. Kurz, K. Lang, T. Maisch, M. Berneburg, Y. Kamenisch, Investigation of the HelioVital filter foil revealed protective effects against UVA1 irradiation-induced DNA damage and against UVA1-induced expression of matrixmetalloproteinases (MMP) MMP1, MMP2, MMP3 and MMP15, Photochem. Photobiol. Sci. (2022), https://doi.org/10.1007/s43630-022-00177-4.
[47] G.A. Cabral-Pacheco, I. Garza-Veloz, C. Castruita-De la Rosa, J.M. Ramirez-Acuña, B.A. Perez-Romero, J.F. Guerrero-Rodriguez, N. Martinez-Avila, M.L. Martinez-Fierro, The roles of matrix metalloproteinases and their inhibitors in human diseases, Int. J. Mol. Sci. 21 (2020) 9739. https://www.mdpi.com/1422-0067/21/24/9739.
[48] X. Zhou, J. Yan, Q. Lu, H. Zhou, L. Fan, The pathogenesis of cutaneous lupus erythematosus: the aberrant distribution and function of different cell types in skin lesions, Scand. J. Immunol. 93 (2021) e12933, https://doi.org/10.1111/sji.12933.
[49] A.S. Frolova, A.I. Petushkova, V.A. Makarov, S.M. Soond, A.A. Zamyatnin Jr., Unravelling the network of nuclear matrix metalloproteinases for targeted drug design, Biology 9 (2020), https://doi.org/10.3390/biology9120480.
[50] M. Maldonado, A. Salgado-Aguayo, I. Herrera, S. Cabrera, B. Ortíz-Quintero, C. A. Staab-Weijnitz, O. Eickelberg, R. Ramírez, A.M. Manicone, M. Selman, A. Pardo, Upregulation and nuclear location of MMP28 in alveolar epithelium of idiopathic pulmonary fibrosis, Am. J. Respir. Cell Mol. Biol. 59 (2018) 77–86, https://doi.org/10.1165/rcmb.2017-0223OC.
[51] C.M. Hedrich, B. Fiebig, F.H. Hauck, S. Sallmann, G. Hahn, C. Pfeiffer, G. Heubner, M.A. Lee-Kirsch, M. Gahr, Chilblain lupus erythematosus–a review of literature, Clin. Rheumatol. 27 (2008) 949–954, https://doi.org/10.1007/s10067-008-0942-9.
[52] R.S. Klein, R.M. Sayre, J.C. Dowdy, V.P. Werth, The risk of ultraviolet radiation exposure from indoor lamps in lupus erythematosus, Autoimmun. Rev. 8 (2009) 320–324, https://doi.org/10.1016/j.autrev.2008.10.003.
[53] S. Prasad, J. Coias, H.W. Chen, H. Jacobe, Utilizing UVA-1 phototherapy, Dermatol. Clin. 38 (2020) 79–90, https://doi.org/10.1016/j.det.2019.08.011.
[54] A. Pérez-Sánchez, E. Barrajón-Catalán, M. Herranz-López, V. Micol, Nutraceuticals for skin care: a comprehensive review of human clinical studies, Nutrients 10 (2018) 403. https://www.mdpi.com/2072-6643/10/4/403.
[55] M. Meinhardt, R. Krebs, A. Anders, U. Heinrich, H.P.D. Tronnier, Wavelength-dependent penetration depths of ultraviolet radiation in human skin, J. Biomed. Opt. 13 (4) (2008) 044030, https://doi.org/10.1117/1.2957970.
[56] S. DelOlmo-Romero, I. Medina-Martínez, R. Gil-Gutierrez, G. Pocovi-Gerardino, M. Correa-Rodríguez, N. Ortego-Centeno, B. Rueda-Medina, Metabolic syndrome in systemic lupus erythematosus patients under Mediterranean diet, Med. Clin. 162 (2024) 259–264, https://doi.org/10.1016/j.medcli.2023.10.009.
[57] C.C. Mok, Metabolic syndrome and systemic lupus erythematosus: the connection, Expert Rev. Clin. Immunol. 15 (2019) 765–775, https://doi.org/10.1080/1744666X.2019.1620601.
[58] H. Xia, J. Chen, H. Gao, S.N. Kong, A. Deivasigamani, M. Shi, T. Xie, K.M. Hui, Hypoxia-induced modulation of glucose transporter expression impacts 18F-fluorodeoxyglucose PET-CT imaging in hepatocellular carcinoma, Eur. J. Nucl. Med. Mol. Imag. 47 (2020) 787–797, https://doi.org/10.1007/s00259-019-04638-4.
[59] D. Choi, J. Kim, J.W. Yang, J.H. Kim, S. Park, J.I. Shin, Dysregulated MicroRNAs in the pathogenesis of systemic lupus erythematosus: a comprehensive review, Int. J. Biol. Sci. 19 (2023) 2495–2514, https://doi.org/10.7150/ijbs.74315.